

Lizette Morejón Alonso^a, José Ángel Delgado García-Menocal^a, Maite García-Vallés^b, Salvador Martínez Manent^b, Elizabeth Rosado Balmayor^c, Martijn van Griensven^c

^aCenter of Biomaterials, University of Havana, Havana, Cuba

^bFaculty of Earth Sciences, University of Barcelona, Barcelona, Spain

^cTechnical University of Munich, Munich, Germany

Exploring the use of silica sands and calcite from natural deposits to prepare bioactive glasses

Paper presented at the “VII International Congress of Biomaterials, BIOMAT’18”, 14–16 March 2018, Havana, Cuba

Nowadays bioactive glasses represent one of the most successful bioceramics used for bone tissue restorations. In this work, three types of silica sands (White, Yellow and Gray sands) and calcite from Cuban natural deposits were employed to synthesize glasses from the system $\text{SiO}_2\text{--CaO--Na}_2\text{O}$. The ions released from glasses were evaluated through in vitro tests in Tris-HCl and in simulated body fluids. All sands had purity around 99.2 % of SiO_2 and contained traces (ppm) of Zr, Cr, Ba, Ce and Sr ions, while calcite raw material had traces of Sr, Cr, Zr, Ce and Zn. All glasses induced a *pH* change in Tris-HCl from 7.4 to 9 after 24 h; they had similar ion-release behavior in the in vitro solutions tested and showed a significant bioactive performance after 5 h. This work illustrates the potentialities of the use of natural resources to develop medical products when recognized trademark materials are not available.

Keywords: Bioactive glasses; Natural raw sources; Bioactivity; Silica sands

1. Introduction

The high incidence of bone injuries due to pathologies or traumas that are reported today by national or international health organizations depicts a challenging medical problem for many surgical services around the world [1–4]. Some bone diseases lead directly to pain or deformity, but others are “silent” disorders until they cause fractures [5]. Injuries of bone tissues can disable and/or impair temporally or permanently the overall style of life of patients and can even put peoples’ lives at severe risk. These circumstances attract the attention of researchers from different branches of knowledge, including surgeons, hospital institutions and health system managers in multiple countries. The usual management of this type of lesions involves surgical treatments that enable the restoration of osseous tissues, which implies significant healthcare resource utilization and hospital costs [6–8].

Bioactive glasses constitute at present one of the most studied biomaterials as bone substitute materials [9]. Their

ability to bond intimately to bone through a layer of hydroxycarbonateapatite (HCA) during the osseointegration process favors the rapid restoration of the bone bed and makes them suitable for a wide variety of clinical applications [10].

The exchange of ions that occurs between medical glasses and body fluids determines both the speed at which biodegradation occurs and its extent. The mechanism that explains the stages by which the HCA layer is generated in silicate-based glass formulations has been described by Hench et al. from Bioglass[®] 45S5 bioactive glass studies [11, 12]. Bioglass[®] 45S5 has been used in multiple clinical applications since the 1980s with encouraging results [13]. Based on the excellent osseointegration behavior of the silicate-based glasses, a wide diversity of bioactive glass formulations has been investigated with the purpose of adjusting their biodegradation rate at the speed of natural bone restoration processes and to satisfy the requirements of specific clinical applications.

However, in developing countries commercialized medical products (as recognized bioactive glasses), are not always available. Facing the imperious clinical necessity of the employment of synthetic biomaterials for bone tissue restorations in severe bone lesions, national health systems develop domestic formulations and study new routes to obtain medical products. For example, a major drawback in large-scale production of bioactive glasses by sol-gel is the high cost of the standard silica precursor, usually tetraethyl orthosilicate (TEOS). In order to evade this problem Adams et al. [14] describe a novel sol-gel preparation of 45S5 bioactive glass using diatom biosilica from cultured cells of the diatom, *Aulacoseira granulata* as substitute for TEOS, and in another work, proposes a bioactive glass in the quaternary system $\text{SiO}_2\text{--Na}_2\text{O--CaO--P}_2\text{O}_5$ from Nigerian sand as the silica source [15]. Additional studies have been targeted to develop bioactive glass ceramics composed of $\text{SiO}_2\text{--CaO--Na}_2\text{O}$ using rice husk ash waste material as a natural source of silica [16, 17].

This work explores the use of Cuban natural resources to obtain silicate-based glasses that can be used for the restoration of injuries of the skeletal system and that can be accessible to the national health system. The usefulness of silica sands that are extracted from the Santa Teresa deposit

located in Pinar del Rio Province (Cuba) and the calcite deposit in Jaruco, in the Mayabeque Province (Cuba) and their potential for the manufacture of bioglass, was investigated.

Previous works of our research group have shown that it is possible to obtain glasses with compositions very close to the zone of the primary crystallization of the combeite phase ($\text{Na}_2\text{O} \cdot 2\text{CaO} \cdot 3\text{SiO}_2$) in the ternary diagram and that they possess bioactive behavior, which is a prerequisite for those biomaterials that are designed for the replacement of bone tissue [18]. However, due to the diversity of sands that can make up the mineral deposit, it is vital to carry out a systematic study to establish if all the materials of the deposit have the same potentialities.

The Santa Teresa silica sand deposit is located in the southwest of Pinar del Río Province in Cuba. It has alluvial origin and is characterized by quartzose sand that remains on the surface, rare times below a reduced vegetation layer (few cm) or without it. According to reports the content of silica (SiO_2), reaches maximum values up to 99.8% averaging around 98.6% [19, 20]. The usable sands appear in a sequence of 1.85 m of average thickness constituted by a gradation of three superimposed layers of colored quartz sand: white, yellow, brown, successively. As a base of the useful sequence, the cutting continues: from 1.85 to 3.80 m with fine yellowish-brown sand, from 3.80 to 4.55 m with sandy-brownish gray-greenish to very dark blue-gray, 4.55 to 11.00 m greenish-gray clay to bluish-blackish brownish brown [19].

In this work, three types of sands from the usable layer of the Santa Teresa deposit and calcite from the Jaruco deposit were evaluated for the synthesis of bioactive glasses. The influence of the differences in the composition of these sands on the process of obtaining the glasses, their final properties such as glass transition temperature, ion exchange rate to simulated media and their bioactive behavior were evaluated.

2. Experimental procedure

2.1. Raw materials

2.1.1. Silica sands

Considering the diversity of sands available in the Santa Teresa deposit, in this work the sands studied were classified according to their appearance in colors: White (WS), Yellow (YS) and Gray (GS) sands. Moreover, White sand was subjected to the treatment called: *Minerals Separation by Dense Liquids* with bromoform to remove heavy metals in order to compare it with the original sand, and it was named: White Treated sand (WTS). In addition, SiO_2 commercial reactive (99.5%, <10 μm , Alfa Aesar, Spain), named: Synthetic sand (SS) was employed to prepare a glass reference. X-ray fluorescence (XRF), infrared spectroscopy (FTIR) and X-ray diffraction (XRD) analyses were performed to characterize these raw materials.

2.1.2. Calcite mineral

Calcite from Jaruco deposit in Mayabeque, Cuba, was characterized by means of XRF, FTIR and XRD.

2.2. Glass synthesis

Glass samples were prepared using silica sands and calcite as natural sources. The materials were sieved to remove foreign inclusions and were manually ground using an agate mortar. Sodium carbonate anhydrous, Na_2CO_3 (99.5%, Applichem Panreac[®], Spain) was added as a flux material and also as a network modifier. A glass synthetic formulation was obtained from pure reagents: SiO_2 (99.5%, <10 μm , Alfa Aesar, Spain), Na_2CO_3 (99.5%, Applichem Panreac[®], Spain) and CaCO_3 (99.0%, Applichem Panreac[®], Spain). The proportions used for all glasses were SiO_2 38.60 wt.%; CaCO_3 30.83 wt.% and NaCO_3 30.56 wt.%.

The reactants were weighed, homogeneously mixed and melted in a Pt-10% Rh crucible using the following heating treatment: they were ramped up to 650 °C at 2 K min⁻¹, ramped up to 950 °C at 1 K min⁻¹, ramped up to 1450 °C at 5 K min⁻¹ and held for 3 h at 1450 °C before the subsequent quench of the melt on preheated stainless steel plates at 400 °C. Finally, the glasses were annealed for 2 h at 450 °C and cooled slowly to eliminate any residual stress. In all cases, translucent glass pieces were obtained.

Taking into account the characterization test to be performed, glass pieces were cut into small blocks or fragments were crushed. The glass powders were sifted between 150–300 μm .

Samples were named according to the type of sand used in their obtaining, e. g. glass from White sand: G-WS.

2.3. Characterization assays

2.3.1. Infrared spectroscopy

Sands and glass powders were characterized by FTIR (Perkin Elmer Spectrum One, USA). About 10 mg of each sample were blended with KBr for IR spectroscopy (Sigma-Aldrich, Germany) and then pressed into translucent pellets for their measurement. Spectra in the 4000–400 cm⁻¹ range were obtained from co-addition of 100 scans.

2.3.2. X-ray diffraction analyses

Powder samples were manually pressed in cylindrical standard sample holders of 16 mm of diameter and 2.5 mm of height. PANalytical X'Pert PRO MPD Alpha1 (Netherlands) powder diffractometer in Bragg-Brentano $\theta/2\theta$ was used to obtain XRD patterns. $\text{Cu-K}_{\alpha 1}$ radiation ($\lambda = 1.5406 \text{ \AA}$) was employed and the measuring was taken from 4 to 80° in 2θ with step size of 0.017°. The XRD pattern was processed using the card numbers of the Joint Committee on Powder Diffraction Standards (JCPDS).

2.3.3. X-ray fluorescence spectrometry

XRF was used to determine the chemical composition of raw materials and glasses synthesized.

Majority elements content assay was realized using a sequential wavelength dispersive X-rays fluorescence spectrometer (WDXRF AXIOS Advanced, PANalytical, Netherlands). The protocol included the preparation of pearls (30 mm in diameter) from dry samples (0.3 g) which were properly grounded and homogeneously mixed with 5.7 g

of lithium tetraborate and 5 mg of lithium iodide as surfactant agent. Fusion was carried out at $\pm 120^\circ\text{C}$ using a radiofrequency induction oven (Perle'X-3, PANalytical, Netherlands). Quantification of the elements took place using a calibration curve made with international reference pearls based on geological samples.

Minority elements content assay was done to determine the presence of As, Ba, Ce, Co, Cr, Cu, Ga, Mo, Nb, Ni, Pb, Rb, Sn, Sr, Th, V, W, Y, Zn, Zr. The content of each element was quantified measuring the fluorescence intensity of sample pastilles by means of a Philips PW 2400 spectrophotometer. Pastilles (40 mm in diameter) were prepared with 6 g of dry sample properly crushed together with 2 ml of a 20% solution of Elvacite 2044 dissolved with acetone, which were pressed by applying a pressure of 200 kN for 60 s in an aluminum capsule with a background of boric acid. A calibration curve based on international reference geological samples in pastilles arrangement was drawn. Possible interferences were considered and potential matrix effects corrected.

2.3.4. Dilatometry tests

As part of the characterization of the glasses, dilatometry tests were also carried out and the glass transition temperatures (T_g) were determined (Inseis, L75 Platinum Series, USA).

2.3.5. In vitro tests

2.3.5.1. Ions released in Tris-HCl solution

Static dissolution experiments were performed to evaluate the glass ions release behavior. The test was performed in freshly prepared tris(hydroxymethyl)amino methane-HCl buffered solution (Tris-HCl), simulating the *in vivo* pH in concordance with the biodegradation test of the ISO 10993-14 standard [21]. A Tris-HCl buffered solution was prepared by dissolving 6.625 g of tris-(hydroxymethyl)aminomethane (Sigma-Aldrich, Germany) in 400 mL of bi-distilled water, adjusting pH at 7.4 ± 0.1 with HCl 1 mol L^{-1} at a temperature of $37 \pm 1^\circ\text{C}$ and the final volume was adjusted to 500 mL.

About 100 mg of sieved glass powders were placed in a polyethylene flask with 5 mL of freshly prepared Tris-HCl solution at $37 \pm 1^\circ\text{C}$, mechanical stirring at 120 rpm was maintained and the pH change over time was measured (CRISON pH meter 507, Spain) during the first 24 h. Experiments were in triplicate for each glass formulation.

On the other hand, 250 mg of sieved glass powders of each glass composition were placed in a polyethylene flask in contact with 25 mL of freshly prepared Tris-HCl solution at $37 \pm 1^\circ\text{C}$ and mechanical stirring at 120 rpm was carried out. Through different time intervals: 2, 5 and 24 h and 2, 3, 4 and 7 days aliquots of 250 μL of each sample were transferred to 25 mL flasks and filled using Tris-HCl buffered solution. Elemental concentrations (Si, Ca, Na, Fe, K, Sr, Ba, Mg, Zn, Ce, Al, Cr, As, Ti, P, Zr) of the soaking solutions were analyzed by inductively coupled plasma-OES spectroscopy (Optima 8300 ICP-OES Spectrometer, USA). The test was in duplicate for each glass sample while ICP-OES analyzes were performed in triplicate. The results were calculated as mean \pm standard deviation.

2.3.5.2. Bioactivity in simulated body fluid

The bioactivity of the formulations was studied by soaking samples in simulated body fluid (SBF) at different periods. The glasses were cut into $0.5 \times 0.5 \times 0.5 \text{ cm}$ specimens using a Buehler ISOMETTM (USA) low speed saw. Samples were polished on all their faces with abrasive paper Buehler numbers: 240, 400 and 1000, and finally, with alumina suspensions of particle size of $0.5 \mu\text{m}$. Afterwards, they were ultrasonically washed with bi-distilled water, with ethanol and finally dried. Three simple blocks of each composition were soaked in $0.22 \mu\text{m}$ filtered fresh solutions of SBF. The SBF was prepared using the Kokubo protocol [22] and the experiment was conducted under static conditions at $37 \pm 1^\circ\text{C}$ maintaining a ratio of Superficial Area of blocks/SBF volume: $1 \text{ cm}^2/10 \text{ mL}$. Sampling took place at different times between 5 h and 21 days. The solution was not replaced during the assay. After soaking, the chemical composition of the solution was analyzed by inductively coupled plasma-OES spectroscopy (Optima 8300 ICP-OES Spectrometer, USA), while the block samples were washed off with ethanol, dried at $37 \pm 1^\circ\text{C}$ for 24 h and stored in a desiccator until used.

Morphology and chemical constituents of the coatings formed on the surface of the pieces were analyzed through field emission scanning electron microscopy and energy dispersive X-ray spectroscopy (FESEM-EDX, JSM-7100F, Japan). Crystalline phases of the superficial layer were evaluated by means of XRD (PANalytical X'Pert PRO MPD Alpha1) in contrast with blank samples. The results were expressed as mean \pm standard error of triplicate determinations.

3. Results and discussion

3.1. Characterization of raw materials

Given the diversity of silica sands that constitute the Santa Teresa deposit, it is essential to have a complete characterization of the chemical composition and structure of the different types of sand that can potentially be used for the manufacture of glasses for medical applications. At first sight the sands have different colors which may correspond to variable concentrations of metallic elements in their composition.

The analyses of majority and minority elements by XRF identified which elements were present in each of them. Table 1 shows the majority elements that constitute the natural sands: White sand, Yellow sand and Gray sand. It is possible to appreciate that the three types of sands are highly rich in their content of silica (SiO_2), in all cases with values higher than 99.2%. The concentrations of other elements expressed as oxides indicate that the so-called White sand (WS) has a greater content of titanium ions, while the Yellow sands (YS) have a greater concentration of iron and aluminum ions. On the other hand, the Gray colored sands (GS) have the highest silica content and the lowest amount of other metallic elements. As a result of the evaluation of the content of minority elements in the sands, it was detected that they contained (in decreasing concentration order) traces (ppm) of the ions: Zr, Cr, Ba, Ce and Sr. Concentration values of potentially harmful elements such as As or

Table 1. Majority elements of natural sands and calcite (wt.%).

Samples	SiO ₂	CaO	Na ₂ O	Fe ₂ O ₃	MnO	TiO ₂	K ₂ O	P ₂ O ₅	Al ₂ O ₃	MgO
WS	99.2 ± 0.1	0.14 ± 0.09	0.09 ± 0.1	0.050 ± 0.005	0.004 ± 0.001	0.220 ± 0.002	0.013 ± 0.001	0.012 ± 0.001	0.07 ± 0.01	0.15 ± 0.04
YS	99.18 ± 0.04	0.034 ± 0.007	0.022 ± 0.001	0.160 ± 0.007	0.003 ± 0.001	0.080 ± 0.002	0.048 ± 0.002	0.0129 ± 0.0004	0.352 ± 0.02	0.107 ± 0.002
GS	99.42 ± 0.09	0.04 ± 0.02	0.033 ± 0.01	0.06 ± 0.02	0.004 ± 0.001	0.156 ± 0.005	0.031 ± 0.006	0.013 ± 0.001	0.13 ± 0.04	0.105 ± 0.007
Calcite	0.25 ± 0.09	57.62 ± 0.07	0.08 ± 0.03	0.050 ± 0.001	0.0051 ± 0.0006	0.007 ± 0.002	0.004 ± 0.001	0.063 ± 0.001	0.068 ± 0.002	0.269 ± 0.005

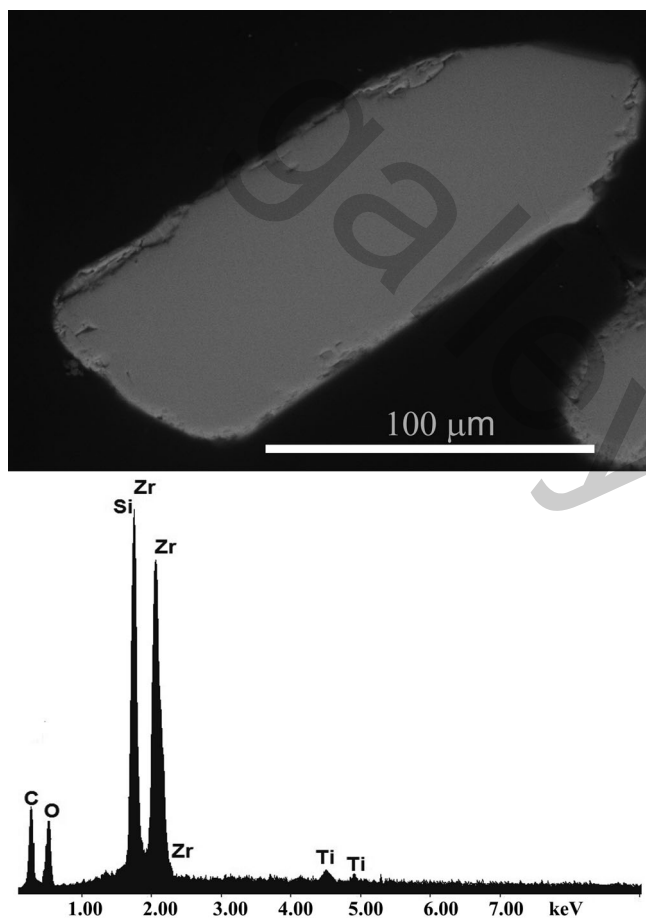
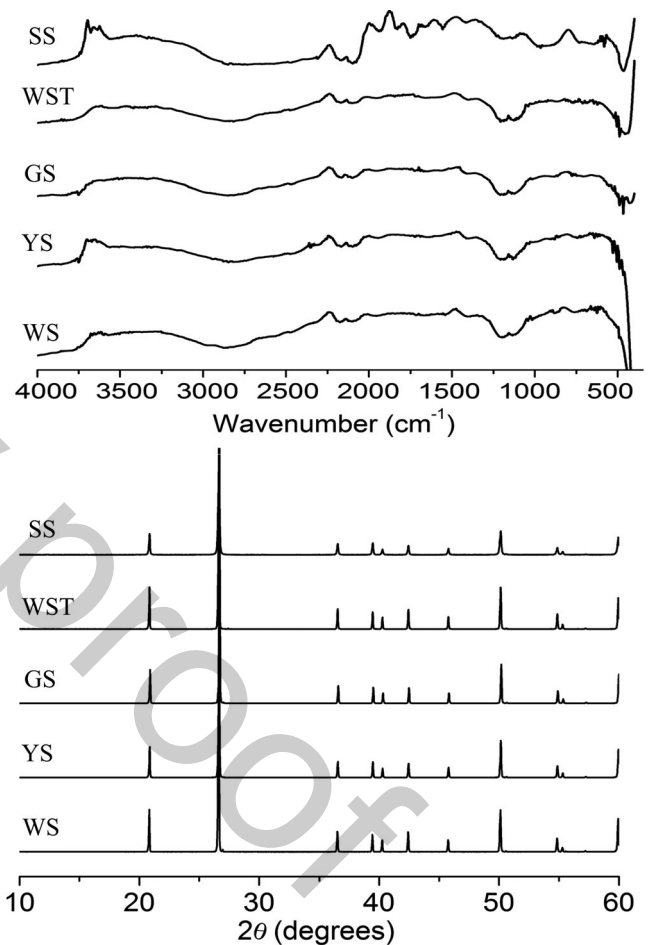
Fig. 1. SEM micrograph and EDX spectrum of zircon crystal (ZrSiO₄) founded in the heavy fraction obtained after mineral separation of the White sand (WS) with bromoform.

Fig. 2. Results of the composition and structural analyses of the sand samples used in the work: (a) FTIR spectra; (b) XRD pattern. Analyses confirm the presence of quartz in the natural sands.

Pb were found in very low ppm values that guarantee that the content of these elements in the subsequent glasses are below the levels established by the ASTM-1538 for glass and glass ceramic biomaterials for implantation [23].

In order to verify the influence of the other metals on the structure of the vitreous material, besides the effect on the rate of ions released and on the bioactivity of the glasses, the white silica sand was subjected to the minerals separation by dense liquids treatment. The heavy fraction was analyzed by SEM-EDX to determine the morphology and elemental composition of the crystals of the separated minerals. The presence in low proportions of zircon

(ZrSiO₄) (Fig. 1), chromite (FeCr₂O₄), barite (BaSO₄), chalcocopyrite (CuFeS₂), pyrite (FeS₂) and ilmenite (FeTiO₃) was detected.

The results obtained from the analysis of the main elements presented in calcite (the second natural source used for the glass synthesis) are summarized in Table 1. The presence of Mg²⁺ ions in significant higher concentration was detected in comparison with the MgO content in the natural sands, while in terms of minority elements the presence of Sr, Cr, Zr, Ce, Zn in ppm (in decreasing concentration order) was also detected.

Figure 2a shows the FTIR spectra of all sands as well as of the reactive silica. Bands between $1200\text{--}1180\text{ cm}^{-1}$ was assigned to the longitudinal optical (LO) modes of the Si-O-Si asymmetric stretching vibrations, bands at the interval of $1128\text{--}1060\text{ cm}^{-1}$ was assigned to the transversal optical (TO) modes of the Si-O-Si asymmetric stretching vibrations, while a weak band around 657 cm^{-1} was assigned to Si-O stretching of the SiO_2 and finally the 468 cm^{-1} band was associated with Si-O symmetrical bending vibration. The detected vibrations reveal the presence of quartz [24]. Figure 2b shows the XRD patterns of the sands which are in total accordance with reflections corresponding to quartz SiO_2 (JCPDS # 01-083-2465).

3.2. Characterizations of glasses

Once the initial characterization of raw materials was completed, the glasses were synthesized and the resulting formulations studied. According to the characterization by XRD all glasses were amorphous. Table 2 shows the composition of the experimental glasses determined by X-ray fluorescence. All formulations were around of 51% SiO_2 -23% CaO -23% Na_2O (in wt.%) and there were no significant changes with the starting nominal composition suggesting that there was no appreciable volatilization. Glasses obtained from natural sources resulted with very similar content of SiO_2 , and the other main elements. Regarding the content of other elements, it is worth noting that glass formulation derived from Yellow sand (G-YS) resulted with the higher content of iron and aluminum in correspondence with the composition of the original sand. The glass obtained from the synthetic silica (reactive silica used to prepare a glass reference) G-SS turned out to be the formulation with more foreign elements, in particular the one with the highest aluminum content.

The dilatometry tests indicated that the vitreous transition temperature (T_g) of all formulations had values between $498\text{--}507^\circ\text{C}$ (Table 3) which indicates that all glasses have a vitreous matrix of a similar nature. Although in the literature there are reports aimed at establishing a model to predict the glass transition temperature of bioactive glasses from their molecular chemical composition, structural aspects such as phase separation, or the presence of intermediate oxide that can act as network modifier oxides, should be taken into account in order to obtain more accurate values in comparison with experimental values of T_g [25, 26].

Table 2. Composition of the experimental glasses (wt.%).

Samples	SiO_2	CaO	Na_2O	Fe_2O_3	MnO	TiO_2	K_2O	P_2O_5	Al_2O_3	MgO
G-WS	51.6 ± 0.1	23.2 ± 0.1	23.56 ± 0.04	0.045 ± 0.005	0.0045 ± 0.0007	0.073 ± 0.002	0.029 ± 0.007	0.039 ± 0.002	0.068 ± 0.017	0.162 ± 0.009
G-YS	51.4 ± 0.2	23.1 ± 0.2	23.5 ± 0.1	0.119 ± 0.002	0.0040 ± 0.0002	0.053 ± 0.001	0.040 ± 0.001	0.0447 ± 0.0004	0.258 ± 0.001	0.171 ± 0.002
G-GS	51.4 ± 0.2	23.1 ± 0.1	23.71 ± 0.02	0.067 ± 0.003	0.0044 ± 0.0004	0.096 ± 0.001	0.026 ± 0.002	0.0414 ± 0.0004	0.080 ± 0.001	0.157 ± 0.001
G-SS	49.9 ± 1.4	22.8 ± 0.7	23.4 ± 0.6	0.057 ± 0.003	0.0027 ± 0.0001	0.0186 ± 0.0002	0.060 ± 0.001	0.044 ± 0.001	0.374 ± 0.014	0.113 ± 0.003
G-WST	51.50 ± 0.01	23.3 ± 0.1	23.58 ± 0.02	0.042 ± 0.003	0.004 ± 0.001	0.043 ± 0.002	0.026 ± 0.003	0.036 ± 0.000	0.056 ± 0.003	0.1603 ± 0.0004

3.2.1. In vitro tests

The use of different metal oxides in the formulations of bioactive glasses responds to the interest of controlling the final properties of vitreous materials with potential applications in medicine. The incorporation of ions with different ionic radius and different valence into the structure influences on the polymerization of the silicate network of the vitreous matrix, as well as the network connectivity.

Properties such as: ion release rate, biodegradation behavior or biocompatibility in vitro and in vivo are strongly influenced by the presence of cations in the vitreous structure. The fact that the silicate network resulted more compact with a greater density of oxygen or remained more expanded due to the presence of a higher non-bridging oxygen content, directly influences on the rate of ion interchange with protons of the dissolution medium and therefore on the rate of ion release and on the rate of the biodegradation process.

3.2.1.1 In vitro test in Tris-HCl solution

In this work, natural sources of sand and calcite were used as raw materials for the glass synthesis. These sources have small contents (almost at trace levels) of different elements that as a whole can modify to a greater or lesser extent important properties of the glasses. Figure 3 summarizes the pH changes that are detected after contacting each glass formulation with Tris-HCl solution. In all cases a rapid increase in pH was detected, which corresponds to the rapid exchange of ions between the vitreous structure and the surrounding medium. All formulations reached pH values very close to 9 after the first 24 h of the test. It was only possible to detect differences between samples in the first 2 h.

Table 3. Glass transition temperature (T_g) of the experimental glasses.

Samples	T_g ($^\circ\text{C}$) \pm SD
G-WS	502.0 ± 0.6
G-YS	505.5 ± 0.3
G-GS	505.2 ± 0.9
G-SS	507.3 ± 0.8
G-WST	498.6 ± 1.2

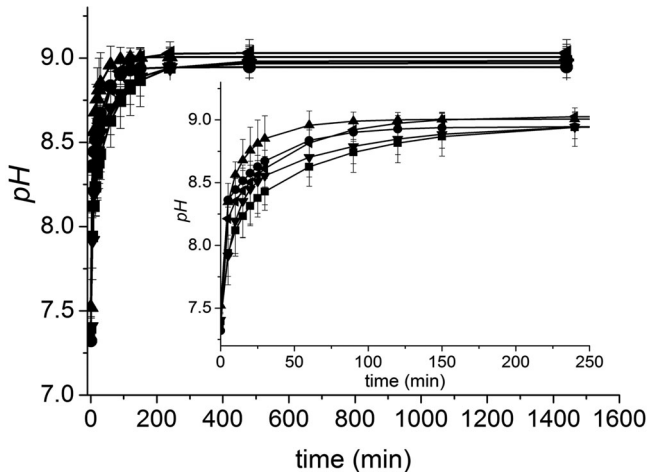


Fig. 3. Variations in pH values after glass immersion in Tris-HCl solution. ■ G-WS, ● G-YS, ▲ G-GS, ▼ G-WST, ◄ G-SS. Values of pH change from 7.4 to 9 for all glasses because of the exchange of ions

In literature, there is extensive evidence on the effect of the use of ions with different ionic radii on the degradation and ion release. The replacement of sodium ions with alkaline ions of smaller radius (for example: Li^+) decreases the ion release in Tris-HCl, while the substitution of sodium by an alkaline ion with a higher ionic radius (for example: K^+) expands the silicate network allowing faster ion release in Tris-HCl solution [27].

The results obtained indicate that the formulation that had the fastest increase in pH was the G-GS, which is the one with a slightly higher Na_2O content of all glasses. This result was because the use of monovalent ions with smaller radius increased the amount of non-bridging oxygens, decreasing network connectivity which favored the ion exchange. Glass samples from White Sand and White Sand Treated (G-WS and G-WST) had the slowest rate of pH increase.

Figure 4 shows the profiles of ion release toward the Tris-HCl solution quantified through ICP-OES. A significant increase of the content of the ions that come from the vitreous structure: Si^{4+} (20–70 mg/L), Ca^{2+} (150–830 mg/L) and Na^+ (180–1030 mg/L) was detected for all glasses. In a first stage the release was quick and later it was slower but sustained at least during the first 7 days. All samples presented similar behavior with no statistical differences.

3.2.1.2 In vitro test in SBF solution

The variation in the content of metal elements in the simulated body fluid was monitored at different times over 21 days after the glasses immersion, Fig. 5. The silicon content increased during the entire period, Fig. 5a. It has been reported in the literature that a rapid exchange of labile ions with H^+ or H_3O^+ from solution to produce silanols (Si-OH) at the glass surface, a loss of soluble silica in the form of Si(OH)_4 and the breaking of the Si-O-Si bonds to form more silanols in bioactive silica-based glasses occur. The condensation of silanols produces a high surface silica gel by partial network dissolution and these surface polycondensation reactions constitute a key step for the bioactivity mechanism [13, 28]. The silica gel layer plays an important

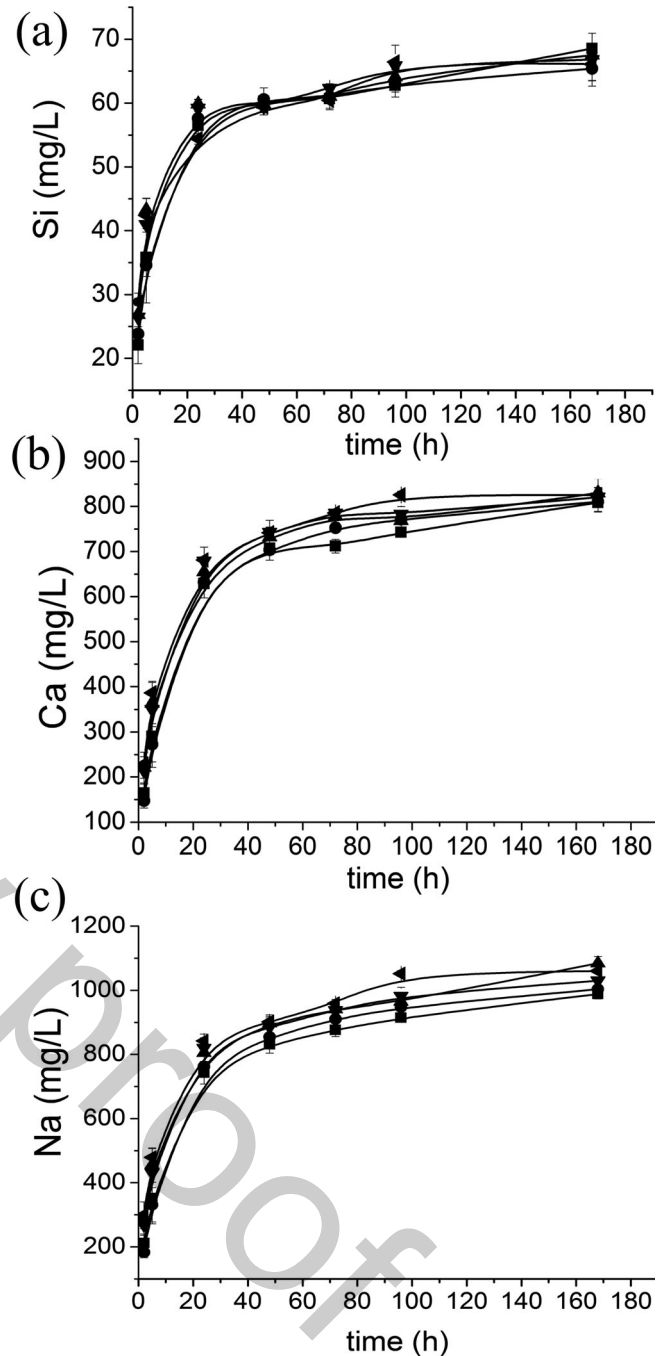


Fig. 4. ICP-OES plots of elemental concentration of (a) Si, (b) Ca, and (c) Na after 7 days of glass immersion in Tris-HCl. ■ G-WS, ● G-YS, ▲ G-GS, ▼ G-WST, ◄ G-SS. No statistical differences were detected between glass samples.

role in the carbonate hydroxyapatite nucleation and crystallization processes.

From Fig. 5b it is clearly observed that the calcium content initially augmented but a posteriori it decreased. A higher concentration of calcium ions increases the degree of the supersaturation of the surrounding body fluid and resulted in the deposition of a calcium-phosphate rich layer on the surface of the glasses. Because of the precipitation of the apatite layer, the SBF initial concentration of phosphorus gradually decreased over time, Fig. 5d. The content of sodium firstly increased but later was sustained over time, Fig. 5c.

The concentrations of the other elements that are in smaller proportions behaved in different ways: for K, Cr and Zn concentrations showed a slight increase in time, for Al, Ti and Ce they oscillated depending on the particular glass sample, for Zr and Mg they remained almost stable, while the Ba concentration decreased slightly, Fig. 5e–g.

SEM micrographs of the glass sample surface reflected significant changes in the topography with time, Fig. 6. Figure 6a–d shows the surface of the glasses after 5 h of immersion in SBF. It was possible to observe the presence of globular aggregates completely covering the surface of the glasses. The aggregates were constituted of many small particles. In the EDX analysis (Table 4) the presence of Si, Na, Ca, P and O was detected, which indicates that the surface layer was extremely thin because of the substrate components were also detected (elements of the vitreous matrix).

In the literature is also reported that the use of multivalent modifying oxides such as Al^{3+} , Zr^{4+} , Ti^{4+} and Ta^{5+} influences the strength of the vitreous network bonds usually constituted by Si-O-Si bonds and partially substituted in the new formulations by Si-O-*Me* links which modifies mechanical properties of the final materials, alters the speed of ion exchange with the environment, influences the bioactivity of the glasses (can even suppress it depending on the amount used) and affects the biodegradation rate [29, 30]. According to the morphological analysis, the surface of the G-SS glass was the one that had globular aggregates of smaller dimensions, which is in correspondence with the formulation with highest Al_2O_3 content. After 24 h more agglomerates and superficial layers with higher thickness for all glass formulations were detected because of the growth of the particles.

After 5 days on the globular agglomerates, the growth of tiny nanometric needles was detected, Fig. 7. Finally, after 21 days (Fig. 6e–h), nanoneedles completely covered the surface of all formulations. According to the EDX analysis (Table 4) for this period, the detectable elements in the sur-

face layer were mainly calcium and phosphorus while the silicon ions of the vitreous matrix were no longer detected.

To elucidate the phase composition of the deposited layer, an XRD study was carried out (Fig. 8). By means of the XRD of the original glasses (Fig. 8a), it was corroborated that they have an amorphous structure with only a widening of the signal between $25\text{--}40^\circ$ in 2θ . However, in the XRD patterns of the surface of the glasses, after soaking the glasses in SBF, new reflections were detected. These new signals correspond to hydroxyapatite (JCPDS # 09-0432), in particular to the crystalline planes (002) and (211) centered approximately in the positions in 2θ , 26 and 32° respectively [30].

These results agree with the predictive studies carried out by Anderson et al. [31] which established a model that correlated the in vivo response of 16 glass formulations implanted in rabbit femur with its chemical composition. The model was applicable to formulations containing oxide concentrations in the following ranges: SiO_2 (38–65 wt.%), CaO (10–24 wt.%), Na_2O (15–30 wt.%), P_2O_5 (0–8 wt.%) B_2O_3 (0–3 wt.%) and Al_2O_3 (0–3 wt.%):

$$RN = 88.3875 - 0.0116272 [\text{SiO}_2]^2 - 0.980188 [\text{Na}_2\text{O}] - 1.12306 [\text{CaO}] - 1.20556 [\text{P}_2\text{O}_5] - 0.560527 [\text{B}_2\text{O}_3] - 2.08689 [\text{Al}_2\text{O}_3]$$

where *RN* is the response to the glasses and is considered an acceptable behavior for values of $RN = 4$, and with tightly bonded implants if $RN > 5$. Bioglass® 45S5 exhibited a value of $RN = 6$. In this work, the final chemical composition of the formulations studied were 51% SiO_2 -23% CaO-23% Na_2O (in wt.%), which satisfies the border conditions of the Anderson et al. model [31]. So, considering this empirical model the expected *RN* values for the synthesized glasses in this work would be 9.8, which justifies the fact that in vitro in a period as short as 5 h of immersion in

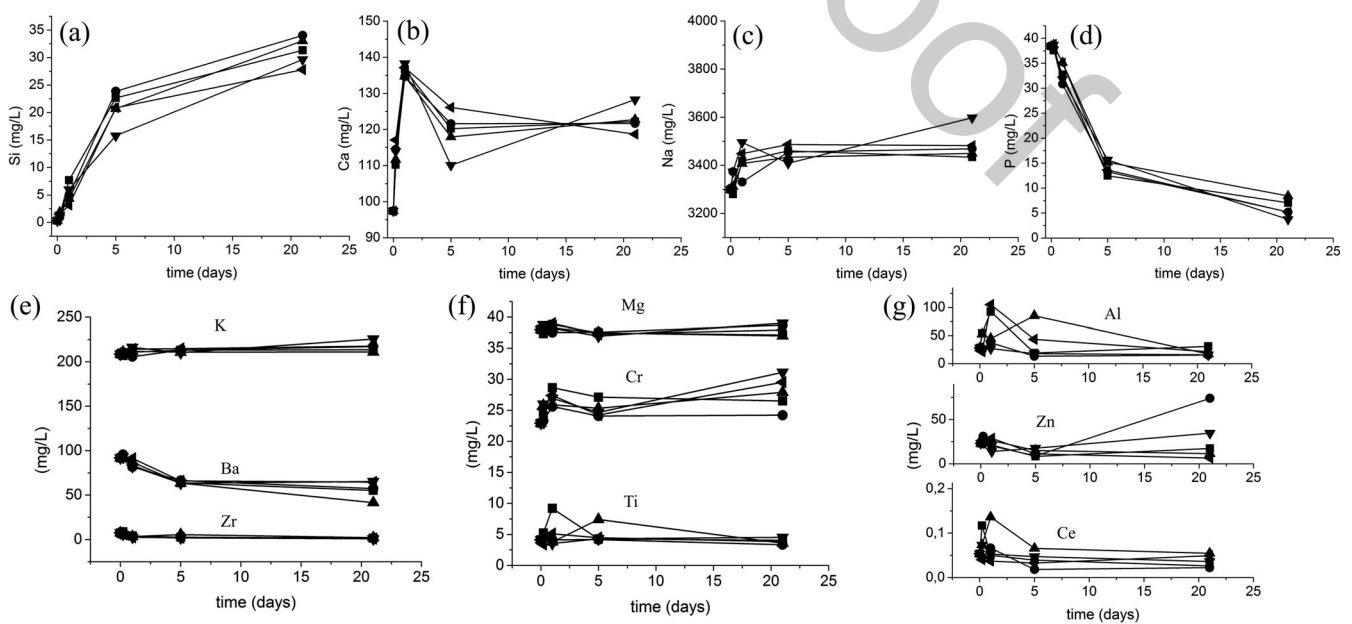


Fig. 5. ICP-OES plots of elemental concentration of SBF after glass soaking in SBF for different time periods. ■ G-WS, ● G-YS, ▲ G-GS, ▼ G-WST, ◀ G-SS. The ion release indicates that Ca ion content firstly increases but with time decreases as the content of P ions, probably because of the deposition of the Ca/P rich layer on glass surfaces.

SBF the entire surface of the glasses was covered with a layer rich in calcium-phosphate corresponding to a hydroxyapatite. The experimental and theoretical results obtained allow assuming that in vivo the glasses studied would be strongly linked to the living bone tissue.

Finally, the comparison of the results of all the studies carried out between the glass formulations obtained from WS and WST did not show substantial behavioral differences. Neither in regard to the chemical composition tests (Table 2), nor by the increase in the pH values that took place after being placed in Tris-HCl (Fig. 3), nor in terms of the release of ions in both Tris-HCl and in SBF (Figs. 4 and 5), besides that they did not show great differences in the study of bioactivity (Fig. 8). These facts support the hypothesis that the sands of the Santa Teresa deposit and the calcite from Jaruco can be used directly for the manufacture of glasses

for clinical applications without significant prior treatments for the removal of heavy metals that they may contain.

For developing countries, it is a great advantage to be able to use their natural resources as mining reserves to obtain products with high added value [32]. The fact that natural sands and calcite can be used directly without prior purification for the manufacture of bioactive glasses constitutes a great alternative since it allows to decrease costs and to obtain higher production volumes. The glasses studied in this work have the potential to be used in various medical specialties that require the replacement of bone tissue, including maxillo-facial surgery or stomatology. In addition, they could be used for the manufacture of composites in combination with other polymeric compounds which would increase the mechanical properties and expand the probable surgical applications.

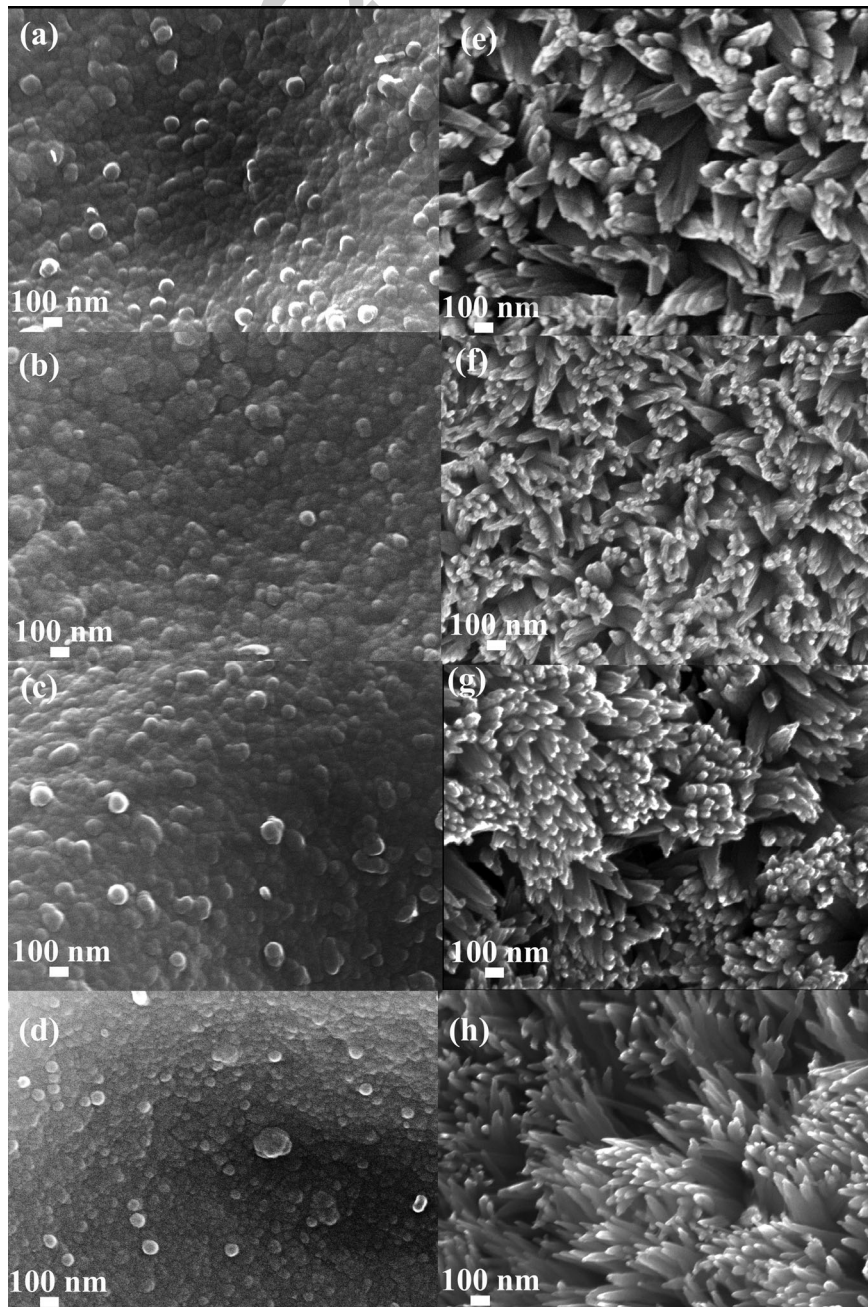


Fig. 6. SEM micrographs of the glass surface after soaking in SBF. (a–d) 5 h after immersion in SBF, globular aggregates of Ca/P deposit were detected covering the surface of all glass compositions; (e–h) 21 days after immersion in SBF, nanoneedles of Ca/P were growing up glass surfaces. (a, e) G-WS; (b, f) G-YS; (c, g) G-GS; (d, h) G-SS.

Table 4. Elemental EDX content of the surface glass samples after soaking in SBF.

Time	Sample	wt. %					Total	Ca/P
		Si	Ca	O	P	Na		
5 h	G-WS	46.11	4.79	47.86	0.9	0.35	100	4.11
	G-YS	40.77	4.46	54.13	0.51	0.13	100	6.76
	G-GS	43.27	4.29	51.17	0.83	0.44	100	3.99
	G-SS	32.21	5.53	61.61	0.39	0.26	100	10.96
	G-WST	38.77	5.11	55.41	0.31	0.4	100	12.74
24 h	G-WS	25.25	12.93	50.74	10.41	0.67	100	0.96
	G-YS	48.04	3.5	44.94	3.01	0.52	100	0.90
	G-GS	49.55	1.93	46.65	1.45	0.42	100	1.03
	G-SS	42.05	3.27	54.15	0.52	0.01	100	4.86
	G-WST	1.51	31.89	47.5	18.51	0.59	100	1.33
21 d	G-WS	–	35.58	43.66	19.85	0.91	100	1.39
	G-YS	–	35.38	44.49	19.59	0.54	100	1.40
	G-GS	–	34.8	45	20.2	–	100	1.33
	G-SS	–	27.03	54.7	17.38	0.9	100	1.20
	G-WST	–	36.85	39.79	22.37	0.99	100	1.27

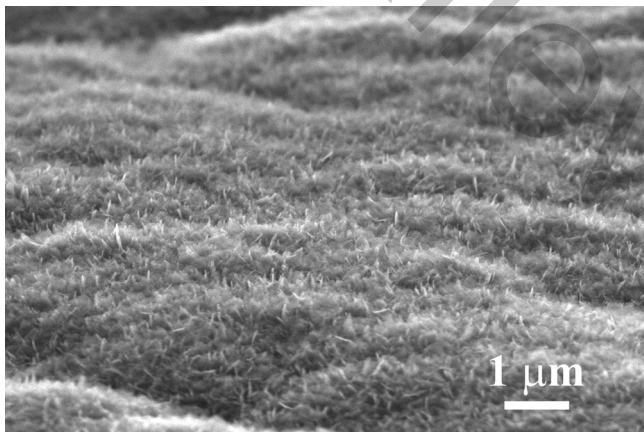


Fig. 7. After 5 days of immersion in SBF of the G-YS the growth of tiny nanometric needles was found on the globular agglomerates.

Other studies that could confirm that the glasses obtained do not involve toxicological risks and have an appropriated biocompatibility should be made in order to complement the evaluation of these formulations. Although other metallic elements are present in the original sands in a very low proportion, the release of their ions to the surrounding medium could have positive (or negative) effects since it is known that some elements, depending on their concentration, participate in physiological processes in the human body. For this reason, new studies should be carried out to establish if sands of a certain color (with specific chemical composition) can generate a more favorable (or unfavorable) response in bone tissue recovery.

4. Conclusions

In this work, different glass formulations obtained from silica sands and natural calcite from Cuban mineral deposits were studied. The studies showed that regardless of the type

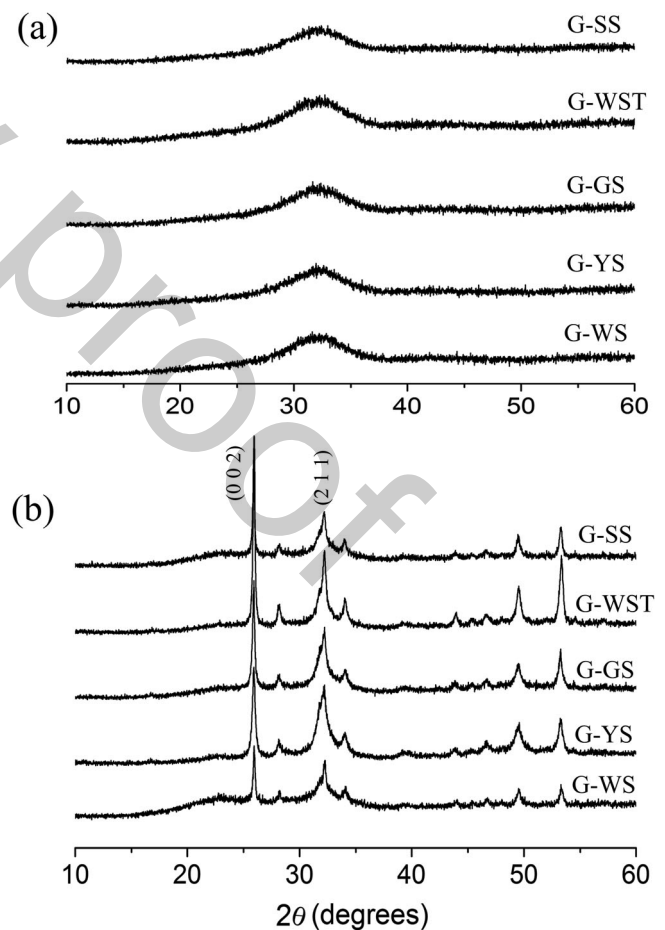


Fig. 8. XRD patterns of the glass surface: (a) Glass blocks before soaking in SBF, (b) Glass blocks after 21 days of being soaked in SBF. Differences were detected between the diffraction patterns of the surface layer of the glasses before and after immersion in SBF. The new reflections detected coincided with the diffraction pattern of hydroxyapatite, which evidenced the bioactivity of the glass formulations studied.

of sand used, similar behavior was obtained in terms of ion release rate and bioactivity behavior from the first five hours in contact with simulated biological fluids. The results obtained show that no prior purification process of the sands is required before the production of the glasses since the behavior results were very similar.

Using natural resources for the manufacture of medical products of high demand in health systems can be an alternative that could contribute to improving the quality of life of patients in developing countries when other options are not available.

The authors acknowledge the financial support provided to L. Morejón during a short term scholarship granted by the Carolina Foundation for its contribution to the obtention of the results of this work. We also thank the Scientific and Technological Centre of the University of Barcelona for analytical data acquisition and Dr. Thomas Hans Aiglsperger for their contribution with the identification tests of the minerals present in the fraction of the treated white sand. The authors also thank the Empresa del Vidrio La Lisa (Cuba) for supplying the raw materials for this study.

References

- [1] M.L. Wolford, K. Palso, A. Bercovitz: NCHS Data Brief, 186 (2015) 1.
- [2] E. Hernlund, A. Svedbom, M. Ivergård, J. Compston, C. Cooper, J. Stenmark, E. McCloskey, B. Jönsson, J. Kanis: Arch Osteoporos 8: 1–2 (2013) 1. DOI:10.1007/s11657-013-0136-1
- [3] T. Vos, A.D. Flaxman, M. Naghavi: The Lancet 380: 9859 (2012) 2163. DOI:10.1016/S0140-6736(12)61729-2
- [4] W. Liang, T. Chikritzh: J. Aging Res. (2016) 1. DOI:10.1155/2016/5071438
- [5] U.S. Department of Health and Human Services. Bone Health and Osteoporosis: A Report of the Surgeon General. Rockville, MD: U.S. Department of Health and Human Services, Office of the Surgeon General, 2004. PMID:20945569
- [6] J.J. Body, I.P. Acklin, O. Gunther, G. Hechmati, J. Pereira, N. Maniadas, E. Terpos, J. Finek, R. von Moos, S. Talbot, H. Sleeboom: J. Bone Oncol. 5 (2016) 185. PMID:28008381; DOI:10.1016/j.jbo.2016.07.003
- [7] D. Weycker, X. Li, R. Barron, R. Bornheimer, D. Chandler: Bone Reports 5 (2016) 186. PMID:28580386; DOI:10.1016/j.bonr.2016.07.005
- [8] J. Félix, V. Andreozzi, M. Soares, P. Borrego, H. Gervásio, A. Moreira, L. Costa, F. Marcelo, F. Peralta, I. Furtado, F. Pina, C. Albuquerque, A. Santos, J.L. Passos-Coelho: Value Health 14 (2011) 499. PMID:21669375; DOI:10.1016/j.jval.2010.11.014
- [9] L.L. Hench, J Mater. Sci-Mater M 17 (2006) 967. PMID:17122907; DOI:10.1007/s10856-006-0432-z
- [10] J.R. Jones, D.S. Brauer, L. Hupa, D.C. Greenspan: Int. J. Appl. Glass Sci. 7: 4 (2016). DOI:10.1111/ijag.12252
- [11] L.L. Hench, R.J. Splinter, W.C. Allen, T.K. Greenlee: J. Biomed. Mater. Res. 2 :1 (1971) 117. DOI:10.1002/jbm.820050611
- [12] L.L. Hench: J. Am. Ceram. Soc. 74 (1991) 1487. DOI:10.1111/j.1151-2916.1991.tb07132.x
- [13] L. L. Hench, in L. L. Hench, J. R. Jones, M. B. Fenn (Eds.), New Materials and Technologies for Healthcare, World Scientific, Singapore (2011) 25. DOI:10.1142/9781848165595_0003
- [14] L.A. Adams, E.R. Essien, A.T. Adesalu, M.L. Julius: J. Sci. Adv. Mater. Dev. (2017),. DOI:10.1016/j.jsamd.2017.09.002
- [15] L.A. Adams, E.R. Essien: Am. J. Biomed. Sci. 7: 4 (2015) 218. DOI:10.5099/aj150400218
- [16] F. Naghizadeh, M.R.A. Kadir, A. Doostmohammadi, F. Roozbahani, N. Iqbal, M.M. Taheri, S.V. Naveen, T. Kamarul: J. Non-Cryst. Solids 427 (2015) 54. DOI:10.1016/j.jnoncrsol.2015.07.017
- [17] S. Kumar: Bachelor of Technology thesis, Sol-gel synthesis and in vitro characterization of bioactive glass ceramics using rice husk ash waste material. National Institute of Technology, Rourkela, Orissa, (2009).
- [18] D. Correa, J.A. Delgado, L. Morejón, N. Brizuela, V.C. Sousa, L.A. dos Santos, Proc. 58° Ceramic Brazilian Congress, Bento Gonçalves, RS, Brazil (2014) 2522.
- [19] https://www.ecured.cu/Yacimiento_de_arena_s%C3%ADlice_Santa_Teresa.
- [20] C.M. Salcines: Tecnología de fundición, Vol 1, Pueblo y Educación, La Habana (1985).
- [21] ISO 10993-14: 2001. Biological evaluation of medical devices. Part 14: Identification and quantification of degradation products from ceramics (ISO 10993-14: 2001).
- [22] T. Kokubo, H. Takadama: Biomaterials 27 (2006) 2907. PMID:16448693; DOI:10.1016/j.biomaterials.2006.01.017
- [23] ASTM F1538-03 (2017), Standard specification for Glass and Glass Ceramic Biomaterials for Implantation, ASTM International, West Conshohocken, PA, 2017.
- [24] Munasir, Triwikantoro, M. Zainuri, Darminto: Mater. Sci.-Poland 33: 1 (2015) 47. DOI:10.1515/msp-2015-0008
- [25] M.D. O'Donnell. Acta Biomater. 7 (2011) 2264. PMID:21256253; DOI:10.1016/j.actbio.2011.01.021
- [26] R.G. Hill, D.S. Brauer: Acta Biomater. 7 (2011) 3601–3605. PMID:21723965; DOI:10.1016/j.actbio.2011.06.023
- [27] R. Brückner, M. Tylkowski, L. Hupa, D.S. Brauer: J. Mater. Chem. B 4 (2016) 312. DOI:10.1039/C5TB02426A
- [28] M. Vallet Regi: J. Chem Soc., Dalton Trans, (2001) 97. DOI:10.1039/b007852m
- [29] M. Navarro, M.P. Ginebra, J. Clement, S. Martínez, G. Avila, J.A. Planell: J. Am. Ceram. Soc. 86: 8 (2003) 1345. DOI:10.1111/j.1151-2916.2003.tb03474.x
- [30] U. Gross, V. Strunz: J. Biomed. Mater. Res., 14: 5 (1980) 607. DOI:10.1002/jbm.820140507
- [31] O.H. Anderson, K.H. Karlsson, K. Kanganiemi: J. Non-Cryst. Solids 119 (1990) 290. DOI:10.1016/0022-3093(90)90301-2
- [32] A.L. Mormul, C.A. Leyva, E. Leyva, R.S. Almenares: Ciencias Holguín, Año XVI (2010) 1.

(Received nix 0, 1900; accepted nix 0, 1900)

Correspondence address

PhD. Lizette Morejón Alonso
Polymeric Biomaterials Department
Center of Biomaterials, University of Havana
Ave. Universidad, e/Ronda y G, Vedado
La Habana 10400
Cuba
Tel. + 53 (7) 8700594
Fax: + 53 (7) 8735863
E-mail: lizette@biomat.uh.cu
lizettemorejon@gmail.com
Web: www.biomat.uh.cu

Bibliography

DOI 10.3139/146.111716
Int. J. Mater. Res. (formerly Z. Metallkd.)
109 (2018) E; page 1–10
© Carl Hanser Verlag GmbH & Co. KG
ISSN 1862-5282